

Global trends and uncertainties in terrestrial denitrification and N₂O emissions

A.F. Bouwman^{a,b}, A.H.W. Beusen^a, J. Griffioen^{c,d}, J.W. Van Groenigen^e, M.M. Hefting^f, O. Oenema^{e,g}, P.J.T.M. Van Puijenbroek^a, S. Seitzinger^h, C.P. Slomp^b, E. Stehfest^a

^a PBL Netherlands Environmental Assessment Agency, P.O. Box 303, 3720 AH Bilthoven, The Netherlands

^b Department of Earth Sciences – Faculty of Geosciences, Utrecht University, PO Box 80021, 3508 TA Utrecht, The Netherlands

^c Department of Innovation, Environmental and Energy Sciences, Faculty of Geosciences, Utrecht University, PO Box 80115, 3508 TA Utrecht, The Netherlands

^d Deltares and TNO Geological Survey of the Netherlands, P.O. Box 85467, 3508 AL Utrecht, the Netherlands

^e Department of Soil Quality, Wageningen University, P.O. Box 47, 6700 AA, Wageningen, The Netherlands

^f Ecology and Biodiversity, Department of Biology, Utrecht University, P.O. Box 800.84, 3508 TB Utrecht, The Netherlands

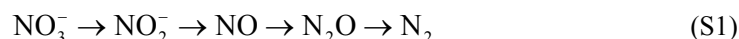
^g Alterra, Wageningen University and Research Center, P.O. Box 47, 6700 AA, Wageningen, The Netherlands.

^h International Geosphere-Biosphere Program, IGBP, Lilla Frescativägen 4a, 11418 Stockholm, Sweden.

Supporting information

S1. Denitrification and N₂O flux measurements

Denitrification is mainly a microbiological process in which nitrate (NO₃⁻) is anaerobically reduced to nitrite (NO₂⁻), nitric oxide (NO), the greenhouse gas nitrous oxide (N₂O) and dinitrogen (N₂):



Soil denitrification rates are generally estimated using indirect methods, because of the near impossibility to measure accurately the increase in N₂ concentration produced by denitrification relative to the high ambient atmospheric N₂ concentration. The conventional method is the measurement of NO₃⁻ disappearance, assuming that this removal is exclusively through denitrification. This is not correct when other loss pathways play a role, for example leaching or NH₃ volatilisation. A second common procedure is the acetylene inhibition technique [1], in which acetylene inhibits the final step in denitrification, and denitrification is assumed to be equivalent to N₂O production. However, this technique can both significantly underestimate [2] or overestimate [3, 4] denitrification rates. A third method makes use of ¹⁵N labelled NO₃⁻ and the measurement of ¹⁵N₂O and ¹⁵N₂. Under controlled conditions, measurements can be made of the increase of N₂O and N₂ following the replacement of the soil atmosphere by helium. A fourth approach is the N-balance method, where the N inputs and outputs for a given area can be measured and, generally, denitrification is the unaccounted for part of the balance. The N balance method generally comprises a prolonged period (for example, a complete growing season). Hofstra and Bouwman [5] showed that the N balance approach generally yields higher denitrification estimates than other techniques. The uncertainty in the determination of each of the terms in the N balance is high and the overall result of the balance is sensitive to minor variation in inputs or outputs, and not always all sources and sinks are taken into account. Finally, under controlled conditions in the laboratory, the end products of denitrification, including N₂, can be measured directly, following replacement of the ambient N₂-rich air in incubation vials with helium (He). However, the results of such controlled-condition experiments are difficult to translate to practical conditions in the field [6].

Generally, the concentration of excess N_2 produced by denitrification in groundwater is estimated by comparing the measured concentrations of Argon (Ar) and N_2 with those expected from atmospheric equilibrium, assuming that Ar is a stable component [7, 8]. Measuring excess N_2 is complicated by variations in recharge temperatures and the entrapment of air bubbles near the groundwater surface, leading to varying background concentrations of dissolved N_2 in groundwater due to contact of the water with atmospheric air [8] or losses by degassing [7]. Local fluxes of N_2O are often measured in vented, closed chambers [9, 10] using a gas chromatograph with ECD detector or with an infrared gas analyser (IRGA) [11-13]. If the flux chambers are attached to pre-installed, permanent frames this will minimize disturbance of the soil structure and reduce errors due to soil compaction and forced diffusion.

S2. The IMAGE model

The objective of the Integrated Model for the Assessment of the Global Environment (IMAGE) version 2.4 model [14] is to explore the long-term dynamics of global environmental change. The model consists of several modules. General economic and demographic trends for 24 world regions drive human activities. Regional energy consumption, energy efficiency improvement, fuel substitution, supply and trade of fossil fuels and renewable energy technologies are simulated with the The IMAGE Energy Regional Model (TIMER) model [15] to calculate energy production, energy use, industrial production, emissions of greenhouse gases, ozone precursors and sulphur. Ecosystem, crop and land-use models are used to compute land use on the basis of regional consumption, technological developments, production and trading of food, animal feed, fodder, grass and timber, and local climatic and terrain properties.

Greenhouse gas emissions from land-use change, natural ecosystems and agricultural production systems are computed as well as the biosphere-atmosphere exchange of carbon dioxide (CO_2). The atmospheric and ocean models calculate changes in atmospheric composition by employing the emissions and by taking oceanic CO_2 uptake and atmospheric chemistry into consideration. Subsequently, changes in climate are computed by resolving oceanic heat transport and changes in radiative forcing by greenhouse gases and aerosols. The ecosystem and crop growth models of IMAGE account for feedbacks of climate change and rising atmospheric CO_2 .

Although IMAGE 2.4 is global in application (with data and scenarios at the scale of world regions), it performs many of its calculations on a terrestrial 0.5 by 0.5 degree resolution (crop yields and crop distribution, land cover, land-use emissions, nutrient surface balances and C cycle). Data from many different sources are used to calibrate the energy, climate and land-use variables over the 1970-2000 period.

Contrary to the original Millennium Ecosystem Assessment (MEA) scenarios described in Alcamo et al. [16] where IMAGE version 2.2 was used [17], here we use an update (version 2.4) of the IMAGE model for simulating land use and nutrient distributions [14]. The major improvements relevant to this study, compared to IMAGE 2.2, include the new land-cover inventory [18], the base year which was updated to the year 2000 (1995 in IMAGE 2.2), the modeling of land-use changes based on a larger number of world regions, an improved description of livestock production systems and the calculation of surface nutrient balances [14].

S3. Scenarios

The four scenarios of the Millennium Ecosystem Assessment (MEA) [16] describe contrasting pathways for the future development of human society and ecosystems. The MEA scenarios are therefore a good basis for expanding them with scenarios for future agricultural nutrient inputs and outputs and nutrient cycling in natural ecosystems. The scenarios are described in comprehensive datasets including greenhouse gas emissions, climate, land use,

etc. Climate data were used by Fekete et al. [19] to compute the runoff fields that, together with land use and climate, form the basis of the calculations in this study.

The Millennium Ecosystem Assessment used four scenarios: Global Orchestration (GO), Order from Strength (OS), Technogarden (TG) and Adapting Mosaic (AM). GO portrays a globally connected society that focuses on global trade and economic liberalisation and takes a reactive approach to ecosystem problems, but also takes strong steps to reduce poverty and inequality and to invest in public goods, such as infrastructure and education.

In contrast, OS is a regionalised and fragmented world, concerned with security and protection, with the emphasis primarily on regional markets, paying little attention to public goods, and taking a reactive approach to ecosystem problems.

TG is a globally connected world relying strongly on environmentally sound technology, using highly managed, often engineered, ecosystems to deliver ecosystem services, and taking a proactive approach to the management of ecosystems in an effort to avoid problems.

In AM, the fourth scenario, regional watershed-scale ecosystems are the focus of political and economic activity. Local institutions are strengthened and local ecosystem management strategies are common; societies develop a strongly proactive approach to the management of ecosystems based on simple technologies. The major drivers relevant to land use and agriculture are discussed below.

Based on the scenario storylines and attitude towards the environment, the regional scenarios for the use of N fertilisers are based on efficiency of N use in crop production (Table S1). This efficiency is the ratio of harvested crop dry matter production to N inputs [20]. For constructing the regional scenarios for fertiliser use, we distinguish countries with a current nutrient surplus (industrialised countries and a number of developing countries like China and India), and countries with a deficit, i.e. the crop uptake exceeds the inputs leading to degradation of soil fertility.

Fertiliser use efficiency is assumed to increase to a varying degree in industrialised countries, China and India, while in most developing countries fertiliser use will increase (with an apparent decrease in fertiliser use efficiency, similar to developments in industrialised countries in the period 1950-1980 [21]) (Table S1).

We used regional data from the FAO Agriculture Towards 2030 study [22] as a guide. Increasing fertiliser use efficiency in industrialised countries is most rapid in the Technogarden and Adapting Mosaic scenarios, based on the attitude towards environmental issues. Also, increasing fertiliser use to avoid soil degradation in developing countries is more important in the Technogarden and Adapting Mosaic scenarios.

The scenarios assume, depending on the economic growth, a gradual increase of livestock production in mixed and industrial systems relative to pastoral systems, leading to increasing amounts of manure stored in animal houses and storage systems.

The scenarios differ in the relative importance of pork and poultry versus ruminant meat, mixed and industrial production, and grazing versus the concentrated feed-dependent production of ruminants. Apart from the impact of such changes on the productivity, the milk and meat production per animal is also assumed to increase; consequently, the excretion per unit of product will decrease. These changes are most rapid in the Global Orchestration and Technogarden scenarios. Improved manure recycling in the total agricultural system is assumed to play an important role in the Adapting Mosaic scenario. Lower meat and milk consumption is a typical feature of the Technogarden scenario compared to the Global Orchestration scenario.

S4. Hydrology

Total runoff is divided into surface runoff and excess water flow:

$$Q_{\text{tot}} = Q_{\text{sro}} + Q_{\text{eff}} \quad (\text{S2})$$

where Q_{sro} is surface runoff (m yr^{-1}), Q_{eff} is the excess water flow from the soil (m yr^{-1}).

Surface runoff is a large part of total runoff in steep areas or in flat terrain with sealed surfaces (e.g. urban areas) or in areas covered with an impermeable topsoil. In our model this is reflected by a slope dependent runoff factor ($f_{\text{Qsro}}(\text{slope})$, no dimension), which is fitted to the slope-runoff classification for unconsolidated sediments according to Bogena et al. [23]:

$$f_{\text{Qsro}}(\text{slope}) = 1 - e^{-0.00617(\text{MAX}[1, S])} \quad (\text{S3})$$

where S is the slope in m km^{-1} , $f_{\text{Qsro}}(\text{slope})$ (no dimension) is the median value within each 0.5 degree grid cell; median value is obtained from 90 by 90 m resolution digital elevation map.

Factors that reduce surface runoff are land use and soil texture [24, 25]. Apart from slope, surface runoff is influenced by soil texture and land use ($f_{\text{Qsro}}(\text{texture})$ and $f_{\text{Qsro}}(\text{landuse})$, respectively, both dimensionless):

$$f_{\text{Qsro}} = f_{\text{Qsro}}(\text{slope}) f_{\text{Qsro}}(\text{texture}) f_{\text{Qsro}}(\text{landuse}) \quad (\text{S4})$$

$$Q_{\text{sro}} = f_{\text{Qsro}} Q_{\text{tot}} \quad (\text{S5})$$

Surface runoff reduction is smallest (10%) in soils with very fine topsoil texture ($f_{\text{Qsro}}(\text{texture})=0.9$), somewhat larger (25%) for loam and sandy loam ($f_{\text{Qsro}}(\text{texture})=0.75$), and and largest (75%) for coarse sand and peat ($f_{\text{Qsro}}(\text{texture})=0.25$). Furthermore, surface runoff is not limited in arable land ($f_{\text{Qsro}}(\text{landuse})=1.0$), reduced by 75% in grassland ($f_{\text{Qsro}}(\text{landuse})=0.25$) and 87.5% in natural vegetation ($f_{\text{Qsro}}(\text{landuse})=0.125$).

After infiltration, groundwater flows laterally to ditches and streams or vertically to deeper groundwater layers. This process is described by distinguishing two groundwater subsystems, similar to Van Dreht et al. [26], De Wit and Pebesma [27] and De Wit [28]. The shallow groundwater system represents the upper 5 metres of the saturated zone and is characterised by short residence times before water enters local surface water at short distances or infiltrates the deep groundwater system.

A deep system with a thickness of 50 m [29] is defined where a deeper ground water flow is present. Deep groundwater is assumed to be absent (i) in areas with non-permeable, consolidated rocks; (ii) in the presence of surface water (rivers, lakes, wetlands, reservoirs); (iii) in coastal lowlands (<5 m above sea level), where we assumed (artificial) drainage or high groundwater levels. This deep groundwater system has longer residence times than the shallow system, as water flows to greater depths and drains to larger rivers at greater distances.

The excess water flow Q_{eff} is divided into interflow (shallow system) and groundwater runoff (deep system):

$$Q_{\text{eff}} = Q_{\text{tot}} - Q_{\text{sro}} = Q_{\text{int}} + Q_{\text{gwb}} \quad (\text{S6})$$

where Q_{int} is interflow through the shallow system (m yr^{-1}), and Q_{gwb} is the groundwater runoff through the deep system (m yr^{-1}). Q_{gwb} is calculated from the fraction f_{Qgwb} of Q_{eff} that flows towards the deep system:

$$Q_{\text{gwb}} = f_{\text{Qgwb}}(p) Q_{\text{eff}} \quad (\text{S7})$$

where p is the effective porosity (-) (Table S2). We assume that the deep layer (if present) has the same soil characteristics as the surface layer.

S5. Soil denitrification

For positive values of the N budget (main text equation 1), denitrification in the top 1 m of soil (or less for shallow soils) is calculated as a fraction $f_{\text{den,soil}}$ [26]:

$$N_{\text{den,soil}} = f_{\text{den,soil}} \text{MAX}(0, N_{\text{budget}} - N_{\text{sro}}) \quad (\text{S8})$$

where N_{sro} is the N loss by surface runoff, calculated on the basis of slope using the approach of Bogaen et al. [23], and further modified by land use and soil texture, i.e. factors that reduce surface runoff according to Velthof et al. [24, 25]:

$$N_{\text{sro}} = f_{\text{Qsro}} C_{\text{sro}} N_{\text{inp}} \quad (\text{S9})$$

where N_{sro} is the N in surface runoff ($\text{kg km}^{-2} \text{yr}^{-1}$), N_{inp} is the N input from fertiliser and animal manure including spreading and grazing, biological N_2 fixation by leguminous crops, atmospheric deposition ($\text{kg km}^{-2} \text{yr}^{-1}$) and f_{Qsro} is the overall runoff fraction (equation S4). C_{sro} (no dimension) is a calibration constant (0.5) so that N_{sro} results match the model of Velthof et al. [24, 25].

$$f_{\text{den,soil}} = \text{MIN}[(f_{\text{climate}} + f_{\text{text}} + f_{\text{drain}} + f_{\text{soc}}), 1] \quad (\text{S10})$$

where f_{climate} (-) represents the effect of climate on denitrification rates, combining the effects of temperature and residence time of water and NO_3^- in the root zone; f_{text} , f_{drain} and f_{soc} (-) (Table S3) are factors representing the effects of soil texture, soil drainage and soil organic C content, respectively. The factor f_{climate} is calculated as:

$$f_{\text{climate}} = f_K T_{\text{r,so}} \quad (\text{S11})$$

where f_K (-) is the temperature effect on denitrification, $T_{\text{r,so}}$ (yr) is the mean annual residence time of water and NO_3^- in the root zone. The temperature effect f_K is calculated according to the Arrhenius equation [30-32]:

$$f_K = 7.94 \cdot 10^{12} \exp\left(\frac{-e_a}{R K}\right) \quad (\text{S12})$$

where e_a is the activation energy (74830 J mol^{-1}), K the mean annual temperature (Kelvin) and R is the molar gas constant ($8.3144 \text{ J mol}^{-1} \text{K}^{-1}$). The mean annual residence time of water in the root zone is given by:

$$T_{\text{r,so}} = \frac{tawc}{Q_{\text{eff}}} \quad (\text{S13})$$

where $tawc$ (m) is the soil total available water capacity for the top 1 m (or less if soils are shallower) and Q_{eff} is defined in equation (S6). We assume that the residence time of NO_3^- equals that of water based on the high mobility of NO_3^- in soils. For agricultural soils under crops in dry regions we assume a minimum value for $T_{\text{r,so}}$ of 1.0; in dry regions agricultural crops can not grow without irrigation, and this is represented by assuming a total water supply equal to the soil water capacity.

This formulation implies that in arid regions residence time is long, resulting in values of f_{climate} and $f_{\text{den,soil}}$ equal to one, suggesting that 100% of the N surplus is removed by denitrification. In arid regions this is not realistic, since there are various fates of N, including accumulation of nitrate in the vadose zone below the root zone [33], surface runoff, ammonia-N volatilisation, nitrification, denitrification [34]. It is not possible to quantify the relative contribution of each process [34], but it is clear that only a negligible part of N surpluses in arid climates is lost by denitrification. We therefore assume that the fate of the N surplus is determined by other processes than denitrification in soils under natural vegetation and grassland and with annual precipitation $< 3 \text{ mm}$. The global amount of this N surplus in the 3100 Mha of arid lands was 20 Tg in the year 2000 (see main text, Figure 4).

The factors for f_{text} , f_{drain} , and f_{soc} account for the soil water and O_2 status (Table S3). Anaerobic conditions favouring denitrification may be more easily reached and maintained for longer periods in fine-textured soils than in coarse-textured ones. This is because fine-textured soils have more capillary pores and hold water more tightly than sandy soils do. The factor f_{drain} accounts for soil aeration, and denitrification rates are generally higher in poorly drained than in well-drained soils [35]. The soil O_2 status is also influenced by root respiration and microbial activity. Oxygen consumption by microorganisms is driven by temperature,

supply of C, and water availability. Temperature and soil water are represented in f_{climate} ; we therefore use soil organic C content as a proxy for the C supply. The values used for f_{text} , f_{drain} and f_{soc} are given in Table S3.

S6. Computing N₂O emissions from soils

Nitrous oxide emission from soils under natural vegetation is calculated with the regression model presented by Bouwman et al. [35]. N₂O emission from fertiliser application and spreading of animal manure in agricultural land are calculated with a regression model based on 846 series of measurements in agricultural fields [36]. The model is based on environmental (climate, soil organic C content, soil texture, drainage and soil pH) and management-related factors (N application rate, fertiliser type, crop type).

S7. Groundwater transport and denitrification

The role of urbanised areas is neglected, because the total area of urbanised land is about 0.3% of the total land area of countries [37]. We note that loss of N to the environment can be substantial in urbanised areas, where sewerage systems are either well-developed or absent [e.g. (38, 39-41)]. The role of natural NH₄ in groundwater is also neglected, which is justified by the observation that the median NH₄ concentration in groundwater of 25 European aquifers is 0.15 mg l⁻¹ [42], which is low (0.7-1.2%) compared to present-day agricultural contamination of groundwater with nitrate, for example in Europe [43].

The difference between the soil N budget, N in surface runoff and denitrification leaches from the root zone to groundwater (if present):

$$N_{\text{leach}} = N_{\text{budget}} - N_{\text{sro}} - N_{\text{den,soil}} \quad (\text{S14})$$

The NO₃⁻ concentration in the excess water leaching from the root zone is calculated from the leached N and the excess water flow (Q_{eff} , equation S6):

$$C_{\text{in}}(0) = \frac{N_{\text{leach}}}{Q_{\text{eff}}} \quad (\text{S15})$$

After infiltration, groundwater flows laterally to ditches and streams or vertically to deeper groundwater layers. The shallow groundwater system represents the upper metres of the saturated zone (typically 5 m) and is characterised by short residence times before water enters local surface water at short distances or infiltrates the deep groundwater system.

We assume that no denitrification occurs in the deep groundwater system. We note that some denitrification could be expected with sedimentary organic matter and pyrite, but also that a bias exists in the literature for sites with rapid denitrification [44], which makes assessment at the global scale difficult.

The NO₃⁻ concentration in groundwater depends on the historical year of infiltration into the saturated zone and the denitrification loss during its transport [8, 26]. Outflow concentrations of N compounds depend on reaction progress. Therefore the time available for denitrification needs to be known. Since we use a time step of one year, seasonal changes in groundwater level are ignored, and mean travel time $T_{\text{r,eq}}$ depends on the ratio between specific groundwater volume and water recharge:

$$T_{\text{r,eq}}(t) = \text{MIN}\left[\frac{pD}{Q_{\text{inflow}}(t)}, 1000\right] \quad (\text{S16})$$

where p is the effective porosity (m³ m⁻³), D is aquifer depth (m) (Table S2) and Q_{inflow} is the water recharge of shallow groundwater, Q_{int} , or recharge of deep groundwater, Q_{gwb} (m y⁻¹). Effective porosity is estimated based on the lithological class (Table S2). The deep system is fed by a vertically draining shallow system (main text, Figure 1). The travel time distribution for vertical flow in the shallow system is uniform so travel time equals mean travel time. For lateral flow to surface water, travel times are highly variable. Meinardi [29] describes travel time distribution for lateral flow in a vertical cross section as follows:

$$g_{age}(z) = -T_{r,aq} \ln(1 - (z / D)) \quad (S17)$$

where z is the depth (m; $z = 0$ at the top and $z=D$ at the bottom of the aquifer), g_{age} is the age of groundwater at depth z (yr), $T_{r,aq}$ is the mean travel time over the thickness of the aquifer (yr). For shallow groundwater (sgrw) we assume $D_{sgrw} = 5$ m, and for the deep groundwater (dgrw) layer (if present) $D_{dgrw} = 50$ m [29].

Denitrification during transport in the shallow system along each flow path in a homogeneous and isotropic aquifer, drained by parallel rivers or streams, is described by a first order degradation process. At time t and at depth z the outflow concentration is:

$$C(t, z) = C_0(t - g_{age}(z)) e^{-k g_{age}(z)} \quad (S18)$$

where the decay rate k is:

$$k = \frac{\ln(2)}{dt50_{den}} \quad (S19)$$

The NO_3^- concentration in the inflow to deep groundwater ($C_0(t)$) is the outflow from the shallow groundwater system. The half-life of NO_3^- in the shallow system $dt50_{den}$ depends on the lithological class [45], with low values (1 year) for silici-clastic material, 2 years for alluvial material, and, 5 years for all other lithological classes. For $dt50_{den} = 2$ and a travel time of 50 years, the NO_3^- concentration will be reduced by $e^{-k(t-50)}$ which is close to 3×10^{-8} .

S8. Denitrification and N_2O emission from riparian areas

For riparian areas, pH is one of the key parameters controlling denitrification rates [46, 47], next to temperature, water saturation, NO_3^- availability and soil organic carbon availability. Under controlled conditions using pure cultures, denitrification activities have been shown to have an optimum at pH 6.5 to 7.5, and decrease at both low (below 4) and high (above 10) pH values.

Our model is based on observed inhibition of denitrification at low soil pH, and the high N_2O fractions when denitrification is inhibited [48, 49]. Hence, the fraction N_2O of total riparian denitrification is high when conditions limit denitrification, and low for optimal conditions for denitrification. Field measurements show a wide range of N_2O emissions from riparian areas (Table S4) indicating that these areas can be both sources and sinks for N_2O . In general, however, fluxes from riparian areas are found to be low compared with agricultural soils. Fractions of N_2O relative to the total denitrification end product ($\text{N}_2 + \text{N}_2\text{O}$) range from 0.3 up to 73% (Table S4).

The denitrification potential in riparian zones is based on the characteristics of the groundwater flow, soil and climate. Denitrification in riparian zones is calculated using the same approach as discussed for soil denitrification; in addition, we assume that heterotrophic denitrification is dominant and is highest at $\text{pH} > 7$ (Figure S1a). A dimensionless denitrification pH reduction factor $f_{denpH,rip}$ is commonly included in denitrification models. This factor assumes a value of 1 at $\text{pH} > 7$ and values of 0 at $\text{pH} < 3$.

$$N_{den,rip} = f_{den,rip} N_{in} \quad (S20)$$

$$f_{den,rip} = \text{MIN}[(f_{climate} + f_{text} + f_{drain} + f_{soc}), 1] f_{denpH,rip} \quad (S21)$$

The N_{in} entering the riparian zone is the residual in the shallow groundwater layer after denitrification has been accounted for. The factor $f_{climate}$ includes the temperature effect f_K (equation S12) and the travel time $T_{r,rip}$ of water and NO_3^- through the riparian zone. $T_{r,rip}$ is calculated as follows:

$$T_{r,rip} = \frac{D_{rip} tawc}{Q_{int}} \quad (S22)$$

where $tawc$ is the available water capacity for the top 1 m, and D_{rip} is the thickness of the riparian zone ($D_{rip} = 0.3$ m of soil, or less for shallow soils), and Q_{int} is the interflow leaving

the shallow groundwater system and flowing through riparian areas. Thus, $T_{r,rip}$ is short where the water flux is large or where the soil layer is thin.

All interflow (if present) in a grid cell is assumed to flow towards streams through riparian zones (main text, Figure 1), except in (fractions of) grid cells with surface water bodies, such as wetlands, lakes or larger streams, where shallow groundwater by-passes riparian zones.

N_2O emission is calculated from the denitrification rate and local soil pH:

$$N_2O_{rip} = f_{den,rip} (1 - f_{den,rip}) f_{N_2OpH,rip} N_{in} \quad (S23)$$

Where $f_{N_2OpH,rip}$ is the fraction N_2O fraction of total denitrification as a function of soil pH (Figure S1b).

S9. Other land based human-managed denitrification

Additional land-based denitrification occurs in manure storage systems, wastewater treatment plants and wetlands. Reliable data on manure storage conditions are not available, particularly for the early 20th century. We assumed that in 1900 all stored animal manure was solid manure, although a fraction of the liquids (urine) may have seeped into the soil. In 2000 and 2050 we assumed that 50% of the stored manure for cattle was solid, and for pigs 20%. This may underestimate the amount of slurries in European countries and other industrialised countries. Denitrification is calculated as 20% of the N in solid manure, accounting for NH_3 losses. Denitrification in manure storage systems thus calculated increased from 2.5 Tg N yr⁻¹ in 1900 to 5 Tg N yr⁻¹ in 2000, and will further increase to up to 10 Tg N yr⁻¹ under the Global Orchestration scenario in 2050.

For wastewater treatment systems we used data from Van Dreht et al. [50] for the period 1970-2050 (Figure S2). Assuming that all N removal is by denitrification, denitrification during wastewater treatment amounted to 2.7 Tg N yr⁻¹ in 2000, and this may increase to up to 12 Tg N yr⁻¹ in 2050 under the Global Orchestration scenario. It is not currently possible for us to estimate denitrification in human-managed wetlands due to a lack of information on how much N is involved.

S10. Sensitivity analysis

The sensitivity of the model to 17 model parameters was investigated for nine output variables representing global results for river N delivery the year 2000 (Table S5). In order to limit computational load in the sensitivity analysis, the Latin Hypercube Sampling (LHS) technique [51] was used. LHS offers a stratified sampling method for the separate input parameters, based on subdividing the range of each of the k parameters into disjunct equiprobable intervals based on a uniform distribution. By sampling one value in each of the N intervals according to the associated distribution in this interval, we obtained N sampled values for each parameter. The number of runs N was 400.

The sampled values for the first model parameter are randomly paired to the samples of the second parameter, and these pairs are subsequently randomly combined with the samples of the third source, etc. This results in an LHS consisting of N combinations of k parameters. The parameter space is thus representatively sampled with a limited number of samples.

LHS can be used in combination with linear regression to quantify the uncertainty contributions of the input parameters to the model outputs [51, 52]. The output Y considered (see columns in Table S6) is approximated by a linear function of the parameters X_i expressed by

$$Y = \beta_0 + \beta_1 X_1 + \beta_2 X_2 \cdots + \beta_n X_n + e \quad (S24)$$

where β_i is the so-called ordinary regression coefficient and e is the error of the approximation. The quality of the regression model is expressed by the coefficient of determination (R^2), representing the amount of variation Y explained by $Y - e$. Since β_i

depends on the scale and dimension of X_i , we used the standardised regression coefficient (SRC), which is a relative sensitivity measure obtained by rescaling the regression equation on the basis of the standard deviations σ_Y and σ_{X_i} :

$$SRC_i = \beta_i \frac{\sigma_{X_i}}{\sigma_Y} \quad (S25)$$

SRC_i can take values in the interval $[-1, 1]$. SRC is the relative change $\Delta Y/\sigma_y$ of Y due to the relative change $\Delta X_i/\sigma_{x_i}$ of the parameter X_i considered (both with respect to their standard deviation σ). Hence, SRC_i is independent of the units, scale and size of the parameters, and thus sensitivity analysis comes close to an uncertainty analysis. A positive SRC_i value indicates that increasing a parameter value will cause an increase in the calculated model output, while a negative value indicates a decrease in the output considered caused by a parameter increase.

The sum of squares of SRC_i values of all parameters equals the coefficient of determination (R^2), which for a perfect fit equals 1. Hence, SRC_i^2/R^2 yields the contribution of parameter X_i to Y . For example, a parameter X_i with $SRC_i = 0.1$ adds 0.01 or 1% to Y in case R^2 equals 1.

Supporting information

Figure captions

Figure S1. (a) Reduction fraction ($f_{\text{denpH,rip}}$) of riparian denitrification as a function of soil pH and (b) the fraction N_2O of total denitrification as a function of soil pH ($f_{\text{N}_2\text{OpH,rip}}$).

Figure S2. Nitrous oxide emission computed for the year 2000 for (a) soils, (b) groundwater and (c) riparian zones. Emissions are denoted in $\text{N}_2\text{O-N}$ per grid cell, because the location of out gassing for groundwater and riparian zones is not known.

Figure S3. Global human N excretion and N removal in wastewater treatment systems for 1970-2000, and 2000-2050 for the four Millennium Ecosystem Assessment scenarios. Based on Van Dreht et al. [26]

References

1. Ryden JC, Lund LJ, Focht DD. Direct in-field measurement of nitrous oxide flux from soils. *Soil Science Society of America Journal*. 1978;42:731-7.
2. Bollmann A, Conrad R. Enhancement by acetylene of the decomposition of nitric oxide in soil. *Soil Biology and Biochemistry*. 1997;29(7):1057-66.
3. Schmidt I, Bock E, Jetten MSM. Ammonia oxidation by *Nitrosomonas eutropha* with NO₂ as oxidant is not inhibited by acetylene. *Microbiology-Sgm*. 2001;147:2247-53.
4. Wrage N, Velthof GL, Oenema O, Laanbroek HJ. Acetylene and oxygen as inhibitors of nitrous oxide production in *Nitrosomonas europaea* and *Nitrosospira briensis*: a cautionary tale. *Fems Microbiology Ecology*. 2004;47(1):13-8.
5. Hofstra N, Bouwman AF. Denitrification in agricultural soils: Summarizing published data and estimating global annual rates. *Nutrient Cycling in Agroecosystems*. 2005;72:267-78.
6. Qin S, Hu C, Oenema O. Quantifying the underestimation of soil denitrification potential as determined by the acetylene inhibition method. *Soil Biology and Biochemistry*. 2012;47:14-7.
7. Blicher-Mathiesen G, McCarty GW, Nielsen LP. Denitrification and degassing in groundwater estimated from dissolved dinitrogen and argon. *Journal of Hydrology*. 1998;208(1-2):16-24.
8. Böhlke J-K, Wanty R, Tuttle M, Delin G, Landon M. Denitrification in the recharge area and discharge area of a transient agricultural nitrate plume in a glacial outwash sand aquifer, Minnesota. *Water Resources Research*. 2002;38(7):10-1 to -26 (doi:10.1029/2001WR000663).
9. Hutchinson GL, Livingston GP. Vents and seals in non-steadystate chambers used for measuring gas exchange between soil and the atmosphere. *European Journal of Soil Science*. 2001;52:675-82.
10. Levy PE, Gray A, Leeson SR, Gaiawyn J, Kelly MPC, Cooper MDA, Dinsmore KJ, Jones SK, Sheppard LJ. Quantification of uncertainty in trace gas fluxes measured by the static chamber method. *European Journal of Soil Science*. 2011;62:811-21.
11. Paul BK, Lubbers IM, Van Groenigen JW. Residue incorporation depth is a controlling factor of earthworm-induced nitrous oxide emissions. *Global Change Biology*. 2012;18(3):1141-51.
12. Alluvione F, Bertora C, Zavattaro L, Grignani C. Nitrous oxide and carbon dioxide emissions following green manure and compost fertilization in corn. *Soil Science Society of America Journal*. 2010;74(2):384-95.
13. Velthof GL, Brader AB, Oenema O. Seasonal variations in nitrous oxide losses from managed grasslands in The Netherlands. *Plant and Soil*. 1996;181:263-74.
14. Bouwman AF, Kram T, Klein Goldewijk K, editors. Integrated modelling of global environmental change. An overview of IMAGE 2.4. Bilthoven: Publication 500110002/2006, Netherlands Environmental Assessment Agency; 2006.
15. Van Vuuren DP, Van Ruijven B, Hoogwijk MM, Isaac M, de Vries HJM. TIMER 2: Model description and application. In: Bouwman AF, Kram T, Klein Goldewijk K, editors. Integrated modelling of global environmental change. Bilthoven: Netherlands Environmental Assessment Agency; 2006. p. 39-59.
16. Alcamo J, Van Vuuren D, Cramer W. Changes in ecosystem services and their drivers across the scenarios. In: Carpenter SR, Pingali PL, Bennett EM, Zurek MB, editors. *Ecosystems and human well-being: scenarios*. Washington, D.C.: Island Press; 2006. p. 279-354.
17. IMAGE-team. The IMAGE 2.2 implementation of the SRES scenarios. A comprehensive analysis of emissions, climate change and impacts in the 21st century. Bilthoven: National Institute for Public Health and the Environment, 2001 CD-ROM publication 481508018; reprinted by Netherlands Environmental Assessment Agency (MNP) as CD-ROM publication 500110001.

18. Klein Goldewijk K, Van Drecht G, Bouwman AF. Contemporary global cropland and grassland distributions on a 5 by 5 minute resolution. *Journal of Land Use Science*. 2006;2:167 - 90, DOI: 10.1080/17474230701622940.
19. Fekete BM, Wisser D, Kroeze C, Mayorga E, Bouwman AF, Wollheim WM, Vörösmarty CJ. Millennium ecosystem assessment scenario drivers (1970-2050): Climate and hydrological alterations. *Global Biogeochemical Cycles*. 2011;24, GB0A12, doi:10.1029/2009GB003593.
20. Bouwman AF, Beusen AHW, Billen G. Human alteration of the global nitrogen and phosphorus soil balances for the period 1970-2050. *Global Biogeochemical Cycles*, 23, doi:10.1029/2009GB003576. 2009.
21. Dobermann A, Cassman KG. Cereal area and nitrogen use efficiency are drivers of future nitrogen fertilizer consumption. *Science in China Ser C Life Sciences*. 2005;48 Supp 1-14.
22. Bruinsma JE. *World agriculture: towards 2015/2030. An FAO perspective*. London: Earthscan; 2003. 432 p.
23. Bogaen H, Kunkel R, Schobel T, Schrey HP, Wendland F. Distributed modeling of groundwater recharge at the macroscale. *Ecological Modelling*. 2005;187(1):15-26.
24. Velthof GL, Oudendag D, Witzke HP, Asman WAH, Klimont Z, Oenema O. Integrated assessment of nitrogen losses from agriculture in EU-27 using MITERRA-EUROPE. *Journal of Environmental Quality*. 2009;38(2):402-17.
25. Velthof GL, Oudendag DA, Oenema O. Development and application of the integrated nitrogen model MITERRA-EUROPE. Wageningen: Alterra, Wageningen UR, The Netherlands; EuroCare, University of Bonn, Germany; ASG, Wageningen UR, The Netherlands, 2007.
26. Van Drecht G, Bouwman AF, Knoop JM, Beusen AHW, Meinardi CR. Global modeling of the fate of nitrogen from point and nonpoint sources in soils, groundwater and surface water. *Global Biogeochemical Cycles*. 2003;17, 1115, doi:10.129/2003GB002060.
27. de Wit M, Pebesma E. Nutrient fluxes at the river basin scale. II: the balance between data availability and model complexity. *Hydrological Processes*. 2001;15(5):761-75.
28. de Wit MJM. Nutrient fluxes at the river basin scale. I: the PolFlow model. *Hydrological Processes*. 2001;15(5):743-59.
29. Meinardi CR. Groundwater recharge and travel times in the sandy regions of the Netherlands. Bilthoven: National Institute for Public Health and the Environment, 1994 Report 715501004.
30. Firestone MK. Biological denitrification. In: Stevenson FJ, editor. *Nitrogen in agricultural soils*. Madison, Wisconsin: American Society of Agronomy, Crop Science Society of America, Soil Science Society of America; 1982. p. 280-326.
31. Shaffer MJ, Halvorson AD, Pierce FJ. Nitrate leaching and economic analysis package (NLEAP): Model description and application. In: Follet RF, Keeney DR, Cruse RM, editors. *Managing nitrogen for groundwater quality and farm profitability*. Madison, Wisconsin, USA: Soil Science Society of America; 1991. p. 285-322.
32. Kragt JF, de Vries W, Breeuwsma A. Modelling nitrate leaching on a regional scale. In: Merckx RH, Vereecken H, Vlassak K, editors. *Fertilization and the environment*. Leuven, Belgium: Leuven University Press; 1990. p. 340-7.
33. Walvoord MA, Phillips FM, Stonestrom DA, Evans RD, Hartsough PC, Newman BD, Striegl RG. A reservoir of nitrate beneath desert soils. *Science*. 2003;302:1021-4.
34. Peterjohn WT, Schlesinger WH. Nitrogen loss from deserts in the southwestern United States. *Biogeochemistry*. 1990;10:67-79.
35. Bouwman AF, Fung I, Matthews E, John J. Global analysis of the potential for N₂O production in natural soils. *Global Biogeochemical Cycles*. 1993;7:557-97.
36. Bouwman AF, Boumans LJM, Batjes NH. Modeling global annual N₂O and NO emissions from fertilized fields. *Global Biogeochemical Cycles*. 2002;16(4):1080 doi:10.29/2001GB001812.

37. Angel S, Sheppard S, Civco D. The dynamics of global urban expansion. Washington, D.C.: The World Bank, Transport and Urban Development Department (http://siteresources.worldbank.org/INTURBANDEVELOPMENT/Resources/dynamics_urban_expansion.pdf), 2005.
38. Foppen JWA. Impact of high-strength wastewater infiltration on groundwater quality and drinking water supply: the case of Sana'a, Yemen. *Journal of Hydrology*. 2002;263:198-216.
39. Wakida FT, Lerner DN. Non agricultural sources of groundwater nitrate: a review and a case study. *Water Resources*. 2005;39:3-16.
40. Van den Brink C, Frapporti G, Griffioen J, Zaadnoordijk WJ. Statistical analysis of anthropogenic versus geochemical-controlled differences in groundwater composition in the Netherlands. *Journal of Hydrology*. 2007;336:470-80.
41. Nyenje PM, Foppen JW, Uhlenbrook S, Kulabako R, Muwanga A. Eutrophication and nutrient release in urban areas of sub-Saharan Africa – A review. *Science of the Total Environment*. 2010;408:447-55, Doi: 10.1016/j.scitotenv.2009.10.020.
42. Shand P, Edmunds WM. The baseline inorganic chemistry of European groundwater. In: Edmunds WM, Shand P, editors. *Natural groundwater quality*. Oxford: Blackwell; 2008. p. 22-58.
43. EEA. Nitrate concentrations in groundwater between 1992 and 2010 in different geographical regions of Europe (<http://www.eea.europa.eu/data-and-maps/figures/nitrate-concentrations-in-groundwater-between-1992-and-2005-in-different-regions-of-europe-3>). Copenhagen: European Environment Agency; 2013 [cited 2013 6 January].
44. Green CT, Puckett LJ, Bohlke JK, Bekins BA, Phillips SP, Kaufman LJ, Denver JM, Johnson HM. Limited occurrence of denitrification in four shallow aquifers in agricultural areas in the United States. *Journal of Environmental Quality*. 2008;37:994-1009, Doi:10.2134/jeq006.0419.
45. Dürr HH, Meybeck M, Dürr S. Lithologic composition of the Earth's continental surfaces derived from a new digital map emphasizing riverine material transfer. *Global Biogeochemical Cycles*. 2005;19, GB4S10, doi:10.1029/2005GB002515.
46. Simek M, Cooper JE. The influence of soil pH on denitrification: progress towards the understanding of this interaction over the last 50 years. *European Journal of Soil Science*. 2002;53:345-54.
47. Knowles R. Denitrification. *Microbiological Reviews*. 1982;46:43-70.
48. van Cleemput O. Subsoils: chemo- and biological denitrification, N₂O and N-2 emissions. *Nutrient Cycling in Agroecosystems*. 1998;52(2-3):187-94.
49. Van den Heuvel RN, Bakker SE, Jetten MSM, Hefting MM. Decreased N₂O reduction by low soil pH causes high N₂O emissions in a riparian ecosystem. *Geobiology*. 2011;9(3):294-300.
50. Van Drecht G, Bouwman AF, Harrison J, Knoop JM. Global nitrogen and phosphate in urban waste water for the period 1970-2050. *Global Biogeochemical Cycles* 23, GB0A03, doi:10.1029/2009GB003458. 2009.
51. Saltelli A, Chan K, Scott EM. *Sensitivity analysis*. Chichester: Wiley and Sons; 2000.
52. Saltelli A, Tarantola S, Campolongo F, Ratto M. *Sensitivity analysis in practice. A guide to assessing scientific models*. Chichester: Wiley and Sons; 2004.
53. Schipper LA, Cooper AB, Harfoot CG, Dyck WJ. Regulators of Denitrification in an Organic Riparian Soil. *Soil Biology & Biochemistry*. 1993;25(7):925-33.
54. Weller DE, Correll DL, Jordan TE. Denitrification in riparian forests receiving agricultural discharges. *Global wetlands*. 1994:117-31.
55. Jordan TE, Weller DE, Correll DL. Denitrification in surface soils of a riparian forest: Effects of water, nitrate and sucrose additions. *Soil Biology and Biochemistry*. 1998;30(7):833-43.
56. Jacinthe PA, Groffman PM, Gold AJ, Mosier A. Patchiness in microbial nitrogen transformations in groundwater in a riparian forest. *Journal of Environmental Quality*. 1998;27(1):156-64.

57. Walker JT, Geron CD, Vose JM, Swank WT. Nitrogen trace gas emissions from a riparian ecosystem in southern Appalachia. *Chemosphere*. 2002;49(10):1389-98.
58. Dhondt K, Boeckx P, Hofman G, Van Cleemput O. Temporal and spatial patterns of denitrification enzyme activity and nitrous oxide fluxes in three adjacent vegetated riparian buffer zones. *Biology and Fertility of Soils*. 2004;40(4):243-51.
59. Hefting MM, Bobbink R, De Caluwe H. Nitrous oxide emission and denitrification in chronically nitrate-loaded riparian buffer zones. *Journal of Environmental Quality*. 2003;32(4):1194-203.
60. Hefting M, Beltman B, Karssenberg D, Rebel K, Van Riessen M, Spijker M. Water quality dynamics and hydrology in nitrate loaded riparian zones in the Netherlands. *Environmental Pollution*. 2006;139(1):143-56.
61. Hefting MM, Bobbink R, Janssens MP. Spatial variation in denitrification and N₂O emission in relation to nitrate removal efficiency in a N-stressed riparian buffer zone. *Ecosystems*. 2006;9(4):550-63.
62. Oehler F, Bordenave P, Durand P. Variations in denitrification in a farming catchment area. *Agriculture, Ecosystems and Environment*. 2007;120:313-24, doi:10.1016/j.agee.10.007.
63. Mander U, Lohmus K, Teiter S, Uri V, Augustin J. Gaseous nitrogen and carbon fluxes in riparian alder stands. *Boreal Environment Research*. 2008;13(3):231-41.
64. Hopfensperger KN, Gault CM, Groffman PM. Influence of plant communities and soil properties on trace gas fluxes in riparian northern hardwood forests. *Forest Ecology and Management*. 2009;258(9):2076-82.
65. Soosaar K, Mander U, Maddison M, Kanal A, Kull A, Lohmus K, Truu J, Augustin J. Dynamics of gaseous nitrogen and carbon fluxes in riparian alder forests. *Ecological Engineering*. 2011;37(1):40-53.
66. Beaulieu JJ, Tank JL, Hamilton SK, Wollheim WM, Hall RO, Jr., Mulholland PJ, Peterson BJ, Ashkenas LR, Cooper LW, Dahm CN, Dodds WK, Grimm NB, Johnson SL, McDowell WH, Poole GC, Valett HM, Arango CP, Bernot MJ, Burgin AJ, Crenshaw CL, Helton AM, Johnson LT, O'Brien JM, Potter JD, Sheibley RW, Sobota DJ, Thomas SM. Nitrous oxide emission from denitrification in stream and river networks. *Proceedings of the National Academy of Sciences of the United States of America*. 2011;108(1):214-9.
67. Vilain G, Garnier J, Tallec G, Tournebize J. Indirect N₂O emissions from shallow groundwater in an agricultural catchment (Seine Basin, France). *Biogeochemistry*. 2011;1-19.
68. Bouwman AF, Klein Goldewijk K, Van der Hoek KW, Beusen AHW, Van Vuuren DP, Willems WJ, Rufino MC, Stehfest E. Exploring global changes in nitrogen and phosphorus cycles in agriculture induced by livestock production over the 1900-2050 period. *Proceedings of the National Academy of Sciences of the United States of America*, doi/101073/pnas1012878108. 2011.
69. Stehfest E. Modelling of Global Crop Production and Resulting N₂O Emissions. Kassel, Germany: PhD thesis. Universität Kassel; 2006.
70. Stehfest E, Bouwman AF. N₂O and NO emission from agricultural fields and soils under natural vegetation: summarizing available measurement data and modeling of global annual emissions. *Nutrient Cycling in Agroecosystems*. 2006;74:207-28 (DOI 10.1007/s10705-006-9000-7).
71. Berdanier AB, Conant RT. Regionally differentiated estimates of cropland N₂O emissions reduce uncertainty in global calculations. *Global Change Biology*, doi: 101111/j1365-2486201102554x. 2011.
72. IPCC. 2006 IPCC Guidelines for National Greenhouse Gas Inventories. Hayama, Japan: IPCC NGGIP Programme, IPCC-TSU/IGES. Published by the Institute for Global Environmental Strategies (IGES), Hayama, Japan on behalf of the IPCC, 2006.

Table S1. Main drivers of ecosystem change for the Millennium Ecosystem Assessment scenarios from Alcamo et al. [16] and assumptions for agricultural nutrient management.

	Global Orchestration (GO)	Order from Strength (OS)	Technogarden (TG)	Adapting Mosaic (AM)
Brief description	Globalisation, economic development, reactive approach to environmental problems	Regionalisation, fragmentation security, reactive approach to environmental problems	Globalisation, environmental technology, proactive approach to environmental problems	Regionalisation, local ecological management with simple technology, proactive approach to environmental problems
General trends				
World population (billion)	Low 2000: 6.1 2030: 7.7 2050: 8.2	High 2000: 6.1 2030: 8.6 2050: 9.7	Medium 2000: 6.1 2030: 8.2 2050: 8.9	High 2000: 6.1 2030: 8.5 2050: 9.6
Income (annual per capita GDP growth rate)	High 2000-2030: 2.6% yr ⁻¹ 2030-2050: 3.0% yr ⁻¹	Low 2000-2030: 1.6% yr ⁻¹ 2030-2050: 1.3% yr ⁻¹	High 2000-2030: 2.1% yr ⁻¹ 2030-2050: 2.6% yr ⁻¹	Medium 2000-2030: 1.8% yr ⁻¹ 2030-2050: 2.2% yr ⁻¹
Global GHG emissions (Gt C-eq yr ⁻¹)	High 2000: 9.8 2050: 25.6	High 2000: 9.8 2050: 20.3	Low 2000: 9.8 2050: 7.1	Medium 2000: 9.8 2050: 18.0
Global mean temperature increase (°C)	High 2000: 0.6 2030: 1.4 2050: 2.0	High 2000: 0.6 2030: 1.3 2050: 1.7	Low 2000: 0.6 2030: 1.3 2050: 1.5	Medium 2000: 0.6 2030: 1.4 2050: 1.9
Per capita food consumption	High, high meat	Low	High, low meat	Low, low meat
Agricultural trends^a				
Productivity increase	High	Low	Medium-high	Medium
Energy crops	4% of cropland area in 2050	1% of cropland area in 2050	28% of cropland area in 2050	2% of cropland area in 2050
Fertiliser use and efficiency	No change in countries with a surplus; rapid increase in N and P fertiliser use in countries with soil nutrient depletion (deficit)	No change in countries with a surplus; slow increase in N and P fertiliser use in countries with soil nutrient depletion (deficit)	Rapid increase in countries with a surplus; rapid increase in N and P fertiliser use in countries with soil nutrient depletion (deficit)	Moderate increase in countries with a surplus; slow increase in N and P fertiliser use in countries with soil nutrient depletion (deficit); better integration of animal manure and re-cycling of human N and P from households with improved sanitation but lacking a sewage connection.

^aScenarios on the scale of 24 world regions of the IMAGE model; a downscaling procedure is used to construct spatially explicit scenarios with 0.5 by 0.5 degree resolution. When aggregated to the country scale, estimates for fertiliser use and livestock production reflect differences between countries in FAO's Agriculture Towards 2030 [22]; the scenario outcomes vary around the FAO values.

Table S2. Porosity (p), the fraction of excess water flowing to deep groundwater ($f_{Q_{gwb}}(p)$), and the half life of NO_3^- in groundwater ($dt50_{den}$) for different lithological classes.

Lithological class ^a	Porosity (p) $m^3 m^{-3}$	$f_{Q_{gwb}}(p)$ ^b (-)	$dt50_{den}$ Year
1. Alluvial deposits	0.15	0.50	2
2. Loess	0.20	0.67	5
3. Dunes and shifting sands	0.30	1.00	5
4. Non- Semiconsolidated sedimentary	0.30	1.00	5
5. Evaporites	0.20	0.67	5
6. Carbonated consolidated sedimentary	0.10	0.33	5
7. Mixed consolidated sedimentary	0.10	0.33	5
8. Silici-clastic consolidated sediment ^c	0.10	0.33	1
9. Volcanic basic	0.05	0.17	5
10. Plutonic basic	0.05	0.17	5
11. Volcanic acid	0.05	0.17	5
12. Complex lithology	0.02	0.07	5
13. Plutonic acid	0.02	0.07	5
14. Metamorphic rock	0.02	0.07	5
15. Precambrian basement	0.02	0.07	5

^a Lithological classes as defined by Dürr et al. [45].

^b $f_{Q_{gwb}}(p)=p/0.3$, 0.3 being maximum porosity.

^c Weathered shales containing pyrite.

Table S3. Denitrification fractions for soil texture, soil organic carbon and soil drainage

Soil texture class	f_{text} (-)	Soil drainage	f_{drain} (-)	Soil organic carbon content	f_{soc} (-)
Coarse	0.0	Excessively-well drained	0.0	< 1%	0
Medium	0.1	Moderate well drained	0.1	1-3%	0.1
Fine	0.2	Imperfectly drained	0.2	3-6%	0.2
Very fine	0.3	Poorly drained	0.3	6-50%	0.3
Organic	0.0	Very poorly drained	0.4	Organic	0.3

Source: Van Drecht et al. [26]

Table S4. Riparian zone N₂O emission and emission fractions.

Reference	N ₂ O emission kg N ha ⁻¹ y ⁻¹	Fraction (N ₂ O/(N ₂ +N ₂ O)) (-)	Fraction (N ₂ O/N _{input}) (-)
Schipper et al. [53]	6390		
Weller et al. [54]	0.04-0.35		
Jordan et al. [55]	0.016-1.5		0.055
Jacinthe et al. [56]	0.66-11.0		0.0002
Walker et al. [57]	24.2		
Dhondt et al. [58]	-1.8- 1,5		
Hefting et al. [59-61]	2-20	0.08-0.73	0.028-0.058
Oehler et al. [62]	51.6	0.6	
Mander et al. [63]	0.44-7.8		
Hopfensperger et al. [64]	0.079		0.03
Soosaar et al. [65]	0.4-0.7	0.019-0.03	0.003
Beaulieu et al. [66]		0.0-0.5	
Vilain et al. [67]	0.5		

Table S5. Model parameters included in the sensitivity analysis, their symbol and description, equation where they are used, and the standard, minimum, mode and maximum value considered for the sampling procedure.

Symbol	Description	Equation	Distribution ^a	Standard	Min.	Mode	Max.
Q_{tot}	Runoff (total)	S2	U1	1.0	0.9		1.1
$Temp$	Mean annual air temperature	S12	U2	0.0	-1.0		1.0
$N_{\text{budget,grass}}$	N budget in grasslands	1	U1	1.0	0.9		1.1
$N_{\text{budget,crops}}$	N budgets in croplands	1	U1	1.0	0.9		1.1
$N_{\text{budget,nat}}$	N budget in natural ecosystems	1	U1	1.0	0.9		1.1
$f_{Q_{\text{sro}}}$	Overall runoff fraction	S4	U1	1.0	0.9		1.1
$f_{Q_{\text{gwb}}}$	Fraction of Q_{eff} that flows towards the deep system	S7	U1	1.0	0.9		1.1
C_{sro}	Calibration constant for N in surface runoff	S9	U3	0.5	0.4		0.6
$f_{Q_{\text{sro}}}(\text{grass})$	Land-use effect on surface runoff for soils under grassland	S4	T1	0.25	0.0	0.25	0.5
$f_{Q_{\text{sro}}}(\text{crops})$	Land-use effect on surface runoff for soils under crops	S4	T2	1.0	0.75	0.995	1.0
$f_{Q_{\text{sro}}}(\text{nat})$	Land-use effect on surface runoff for soils in natural ecosystems	S4	T3	0.125	-0.05	0.125	0.3
D_{rip}	Thickness of riparian zone	S22	T2	0.3	0.2	0.3	1.0
D_{sgrw}	Thickness of shallow groundwater system	S17	U3	5.0	3.0		7.0
D_{dgrw}	Thickness of deep groundwater system	S17	U3	50.0	30.0		70.0
p	Porosity of aquifer material	S7, S16	U1	1.0	0.9		1.1
$dt50_{\text{den,sgrw}}$	Half-life of nitrate in shallow groundwater	S19	U1	1.0	0.8		1.2
$dt50_{\text{den,dgrw}}$	Half-life of nitrate in deep groundwater	S19	T4	∞	0.0	20.0	40.0

^a Samples values are applied to all grid cells. For sampling, either uniform or triangular distributions are used. A triangular distribution is a continuous probability distribution with lower limit a, upper limit b and mode c, where $a \leq c \leq b$. The probability to sample a point depends on the skewness of the triangle. In the case of $dt50_{\text{den,dgrw}}$, $ac=bc$, and probability to sample a point on the left and right hand side of c is the same. In other cases, for example $f_{Q_{\text{sro}}}(\text{crops})$ is a fraction [0,1], with standard value of 1.0. To achieve a high probability to sample close to 1.0, the triangle is designed with $b=1$ and c is close to 1. For some of the above distributions the expected value is not equal to the standard. Since the calculated R^2 for all output parameters exceeds 0.99, this approach for analyzing the sensitivity is still valid. The distributions used are:

U1. Uniform; values are multipliers for standard values on a grid cell basis.

U2. Uniform; values are added to the standard values on a grid cell basis.

U3. Uniform; values are used as such.

T1. Triangular; values range between 0.125 and 0.5.

T2. Triangular.

T3. Triangular; values range between 0.1 and 0.3.

T4. Triangular; default value represents the mode. Values range between 3 and 40. These values are used to multiply with the standard values of $dt50_{\text{den,sgrw}}$ (because we assume there is no denitrification in deep groundwater in the standard case).

Table S6. Standardized regression coefficient (SRC)^a values representing the relative sensitivity of 9 model variables representing global model results (columns) to variation in 17 parameters (rows, see Table S5)

Parameter	Description	N_{budget}	N_{sro}	$N_{\text{den,soil}}$	N_{leach}	$N_{\text{out,sgrw}}$	$N_{\text{out,dgrw}}$	$N_{\text{in,rip}}$	$N_{\text{bypass,rip}}$	$N_{\text{out,river}}$
Q_{tot}	Runoff (total)			-0.22	0.24	0.31	0.19	0.30	0.31	0.32
$Temp$	Mean annual air temperature			0.50	-0.43	-0.19		-0.19	-0.21	-0.18
$N_{\text{budget,grass}}$	N budget in grasslands	0.33	0.02	0.30	0.21	0.14		0.15	0.10	0.14
$N_{\text{budget,crops}}$	N budgets in croplands	0.65	0.17	0.60	0.54	0.25	0.04	0.25	0.25	0.30
$N_{\text{budget,nat}}$	N budget in natural ecosystems	0.73	0.03	0.47	0.67	0.50	0.14	0.51	0.44	0.50
f_{Qsro}	Overall runoff fraction		0.39	-0.05	-0.11	-0.08		-0.09	-0.03	0.11
f_{Qgwb}	Fraction of Q_{eff} that flows towards the deep system					-0.12	0.27	-0.12	-0.10	-0.05
C_{sro}	Calibration constant for N in surface runoff		0.78	-0.14	-0.20	-0.14		-0.14	-0.06	0.25
$f_{\text{Qsro}}(\text{grass})$	Land-use effect on surface runoff for soils under grassland		0.35	-0.06	-0.10	-0.07		-0.08	-0.03	0.10
$f_{\text{Qsro}}(\text{crops})$	Land-use effect on surface runoff for soils under crops		0.31	-0.04	-0.09	-0.07		-0.08	-0.03	0.08
$f_{\text{Qsro}}(\text{nat})$	Land-use effect on surface runoff for soils in natural ecosystems		0.19	-0.01	-0.07	-0.06		-0.07	-0.03	0.03
D_{rip}	Thickness of riparian zone						0.04			-0.20
D_{sgrw}	Thickness of shallow groundwater system					-0.65	-0.14	-0.64	-0.71	-0.57
D_{dgrw}	Thickness of deep groundwater system						-0.46			-0.09
p	Porosity of aquifer material					-0.17	-0.14	-0.16	-0.18	-0.16
$dt50_{\text{den,sgrw}}$	Half-life of nitrate in shallow groundwater					0.31	0.08	0.31	0.34	0.27
$dt50_{\text{den,dgrw}}$	Half-life of nitrate in deep groundwater		-0.01		0.00	0.01	0.66	0.01	0.01	0.13

^a Cells in with no values represent insignificant SRC values; cells with values show significant SRC, grey colours indicate values $-0.2 < \text{SRC} < 0.2$; green and salmon pink colours indicate values exceeding $+0.2$ and -0.2 , respectively. An SRC value of 0.2 indicates that the parameter concerned has an influence of $0.2^2 = 0.04$ (5%) on the model variable considered.

Table S7. Nitrous oxide emissions for 1900-2000 [68] and 2030 and 2050 for the four Millennium Ecosystem Assessment scenarios [20] according to the IMAGE model.

Year/scenario	Natural ecosystems	Agriculture	Groundwater	Riparian	Energy	Industry	Biomass burning	Rivers	Oceans	Total
1900	6.3	2.4	0.1	0.6	n.d.	n.d.	n.d.	0.1	3.0	12.6
1950	5.4	4.0	0.1	0.6	n.d.	n.d.	n.d.	0.1	3.0	13.2
1970	5.1	5.1	0.2	0.7	0.1	0.7	0.1	0.1	3.0	15.2
2000	4.9	6.4	0.2	0.9	0.2	0.4	0.3	0.2	3.0	16.5
2050-GO	5.3	8.8	0.3	1.1	0.5	0.3	0.2	0.2	3.0	19.7
2050-TG	4.8	9.0	0.2	0.9	0.1	0.1	0.1	0.2	3.0	18.4
2050-AM	5.2	7.7	0.2	0.9	0.4	0.3	0.2	0.2	3.0	18.0
2050-OS	4.9	8.7	0.3	1.0	0.5	0.4	0.2	0.2	3.0	19.1

n.d. = no data. Nitrous oxide emissions expressed as Tg N yr⁻¹.

Table S8. Global estimates of N₂O emission from soils under cropland, grassland and natural vegetation^a.

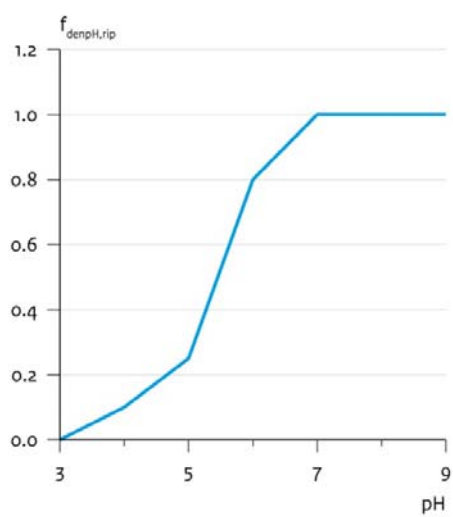
Reference	Cropland	Grassland	Natural ecosystems	Inventory year/model
	N ₂ O-N in Tg yr ⁻¹			
Bouwman et al. [36]	2.7 (1.6-5.1)			1995/statistical
Stehfest [69]	2.1			1998/DAYCENT
Stehfest and Bouwman [70]	3.4 (1.6-6.9)			1995/statistical
Berdanier and Conant [71]	2.3 (1.6-3.2)			1995/statistical
This study	3.2 ^b	2.7	4.9	2000/statistical

^a Excluding N₂O emission of 0.5 Tg N₂O-N yr⁻¹ from animal houses and manure storage systems.

^b Estimates based on IPCC [72]. are not included; IPCC considers the fertiliser-induced emission (emission from fertilised plots minus that from unfertilised control plots) and not the total emissions.

pH effect on denitrification in riparian zones

Denitrification



N_2O

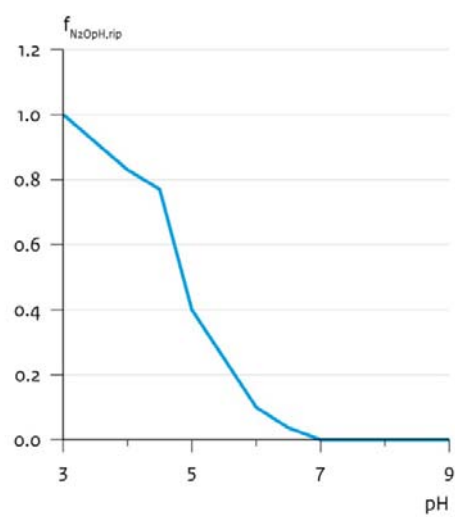


Figure S1.

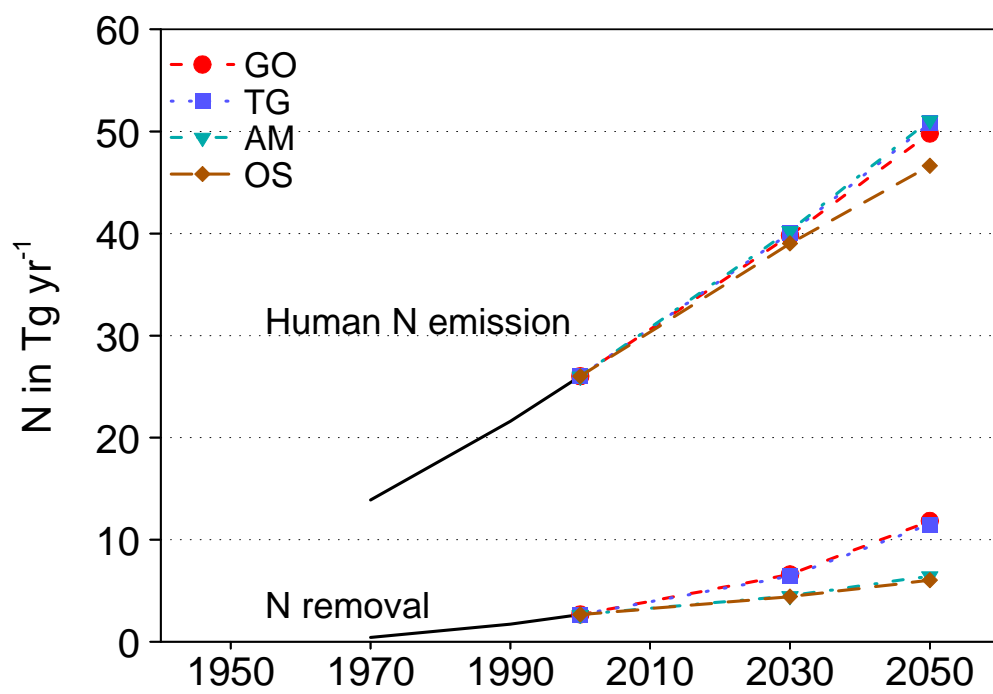
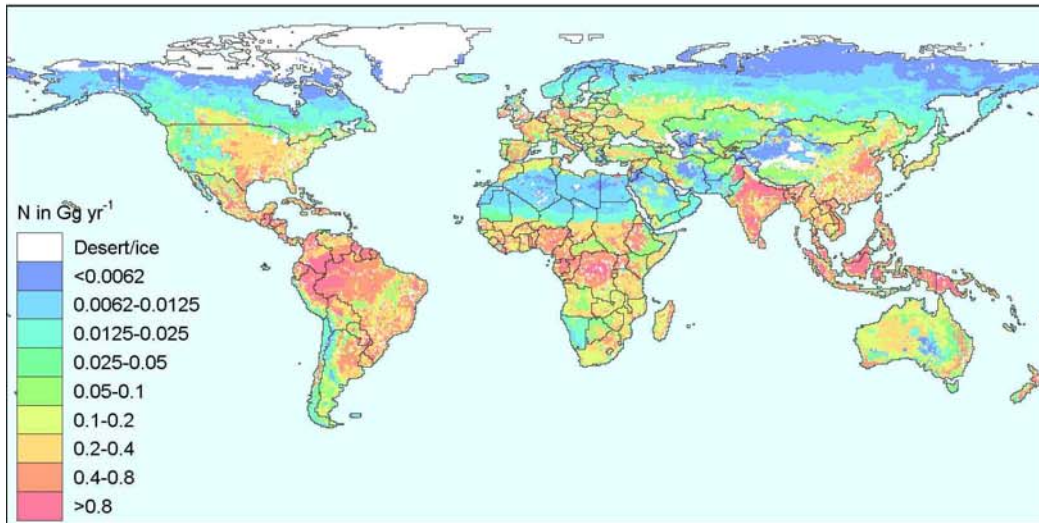
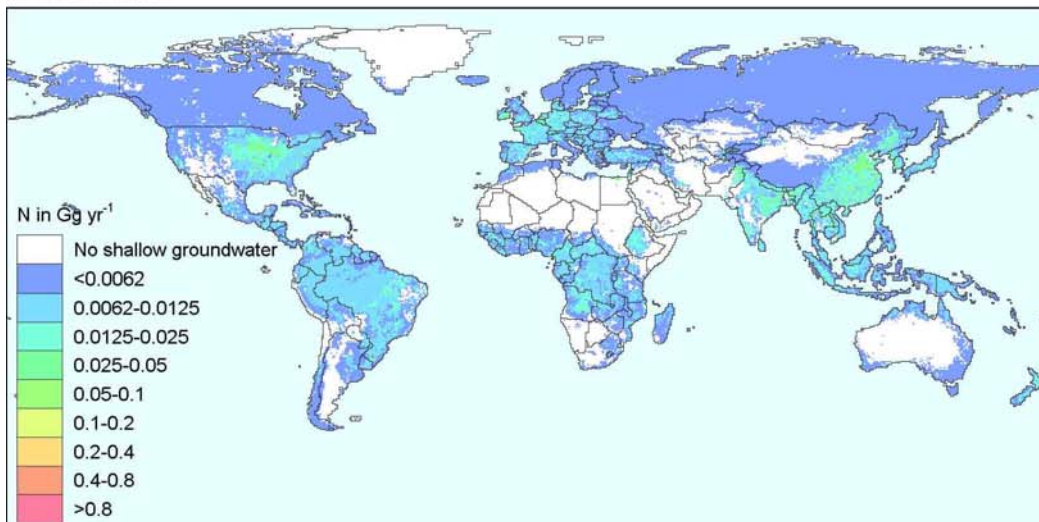


Figure S2.

a. Soil



b. Groundwater



c. Riparian zone

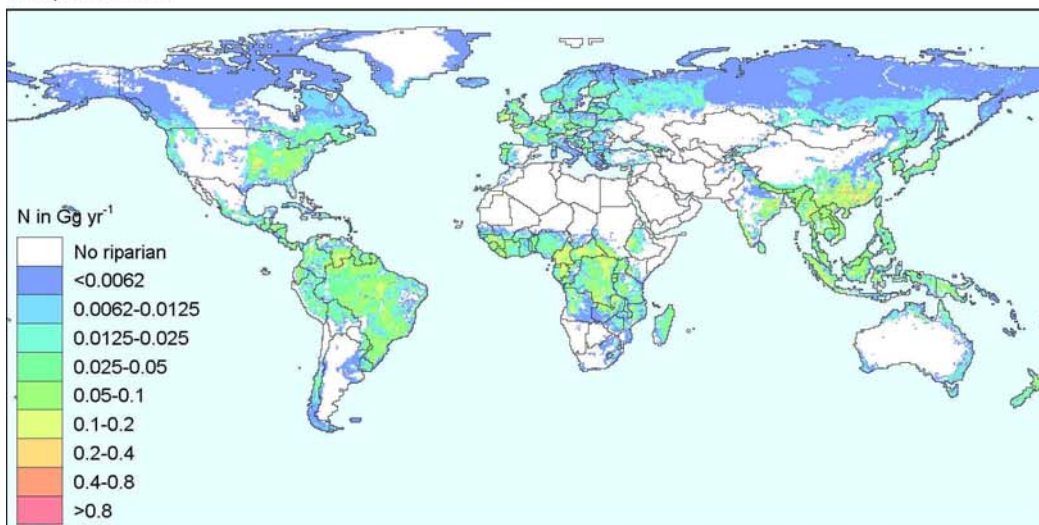


Figure S3.